

See discussions, stats, and author profiles for this publication at: <https://www.researchgate.net/publication/216020079>

# Solvation and ionization of hydroxyl groups in water-ice layers on silver (110)

ARTICLE *in* SURFACE SCIENCE · APRIL 1999

Impact Factor: 1.93 · DOI: 10.1016/S0039-6028(99)00193-4

---

CITATIONS

12

---

READS

15

# Solvation and ionization of hydroxyl groups in water–ice layers on silver (110)

D.S.-W. Lim\*, E.M. Stuve

*Department of Chemical Engineering, University of Washington, Box 351750, Seattle, Washington 98195-1750, USA*

Received 4 August 1998; accepted for publication 4 January 1999

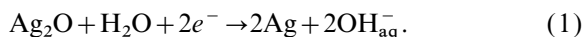
## Abstract

The solvation and ionization of hydroxyl groups on Ag(110) were examined with isotope exchange experiments involving OD and  $^{18}\text{OD}$  and temperature programmed desorption (TPD). Water adsorption onto oxygen-covered Ag(110) gives rise to the well known  $\alpha$ ,  $\beta$ ,  $\gamma$  and  $\delta$  peaks in TPD. The  $\alpha$ -state represents multilayer water, the  $\gamma$  state an  $(\text{OH})_2 \cdot \text{H}_2\text{O}$  complex, and the  $\delta$ -state OH groups. Surface solvation of OH groups involves as many as  $14 \pm 3$  water molecules ( $\beta$  and  $\gamma$ ) in the limit of zero OH coverage and decreases linearly to five water molecules for 0.15 monolayer (ML) of OH. The solvating molecules are essentially all  $\beta$ -state molecules as the  $\gamma$ -state contains only 0.5 water molecules per OH group. The maximum coverage of solvating water molecules and OH groups is 1.04 ML in good agreement with a perfect bilayer coverage of 1.18 ML on Ag(110). From this we identify the  $\beta$ -state as an extended surface bilayer structure. Isotope exchange experiments demonstrated proton mobility in the OD/ $\text{H}_2\text{O}$  adlayer at temperatures of 150 K as well as migration of  $^{18}\text{OD}$  groups from the surface and into  $\alpha$ -state, multilayer water molecules. This constitutes desorption of hydroxide ion into the water–ice multilayers and subsequent solvation. © 1999 Elsevier Science B.V. All rights reserved.

**Keywords:** Chemisorption; Equilibrium thermodynamics and statistical mechanics; Ion–solid interactions; Isotopic exchange/traces; Metal–electrolyte interfaces; Silver; Thermal desorption spectroscopy; Water

## 1. Introduction

Interactions between water and hydroxyl groups are of fundamental interest to areas such as electrochemistry, corrosion and battery technology [1–3]. For example, the cathodic reaction of a zinc/silver oxide battery involves the reaction of water with silver oxide to produce metallic silver and hydroxide ion:



Molecular level details of this reaction, and

many similar ones, are still not well understood. In this work we study the structure and ionic nature of water-hydroxyl adlayers on Ag(110).

Hydroxyl groups are readily formed on Ag(110) by the reaction of water with adsorbed, atomic oxygen [4–13]:



This reaction, which occurs at temperatures as low as 80 K, is general to the late transition and noble metals [14] and, with respect to (110) surfaces, has been studied on Cu [15], Au [16], Pt [17], Pd [18,19] and Ni [19–22]. Strong interactions between water and either hydroxyl groups or

\* Corresponding author. Fax: +1 206 543 3778.

E-mail address: Stuve@u.washington.edu (D.S.-W. Lim)

adsorbed, atomic oxygen are often reported. On Ag(110) hydroxyl groups induce higher temperature desorption states, labelled  $\beta$  (200 K) and  $\gamma$  (240 K). The  $\gamma$ -state corresponds to an  $\text{H}_2\text{O}(\text{OH})_2$  complex [9]. Similar higher temperature desorption states occur for  $\text{H}_2\text{O}/\text{OH}$  on Cu(110), Ni(110) [15] and Pd(110) [18]. Interaction of as many as eight water molecules per OH group was reported on Cu(110) with low OH coverage [15]. Conversely, interaction of only two water molecules per oxygen atom was reported for low oxygen coverages on Pd(110), though interaction of many water molecules per oxygen atom occurred for higher oxygen coverages [18]. LEED studies of the  $\text{H}_2\text{O}/\text{O}/\text{Cu}(110)$  system provide evidence for the existence of long range, through-surface interactions between oxygen and water [15].

The results of the early isotopic exchange experiments of Bowker et al. [23] suggested the possible ionic nature of OH species on Ag(110). They observed exchange between a chemisorbed layer of  $^{18}\text{O}$  and  $\text{H}_2\text{O}$  stabilized by the chemisorbed oxygen (the  $\beta$ ,  $\gamma$  and  $\delta$  states, see below). Based on results from ultraviolet photoemission spectroscopy, Barteau and Madix [6] also suggested that surface OH groups are ionic. In a study of the reaction of water with *molecular* oxygen on Ag(110), Madix and Roberts [10] reported that water multilayers stabilize  $\text{O}_2$  on the surface, shifting its desorption peak from 170 to 200 K. The mechanism for this effect was not identified, but it occurs only in the presence of the multilayer ( $\alpha$ ) state.

Surface adlayers consisting of ionic species like OH and solvent molecules like water are analogous to the near-surface region of an electrode/electrolyte interface [24]. Ionic species in these electrolytic adlayers can either adsorb specifically onto the metal surface or can be fully hydrated depending on the interactions among the metal substrate, water molecules and ionic species. Ion formation in electrolytic adlayers has been observed in several systems under ultrahigh vacuum (UHV) conditions:

1. hydronium ion ( $\text{H}_3\text{O}^+$ ) from coadsorbed H and  $\text{H}_2\text{O}$  on Pt(111) [25] and Pt(100) [26]; and
2. hydrated perchlorate ion ( $\text{ClO}_4^-$ ) from coads-

orbed  $\text{ClO}_4$  and  $\text{H}_2\text{O}$  on Ag(110) [27] and on Au(111) [28].

In the  $\text{H}/\text{H}_2\text{O}/\text{Pt}$  systems, isotope exchange between chemisorbed deuterium and  $\text{H}_2\text{O}$  conclusively proved the existence of hydronium ion, and the presence of a vibrational band at  $1150\text{ cm}^{-1}$  provided further confirming evidence [25,26]. In the case of perchlorate, the presence of non-specifically adsorbed  $\text{ClO}_4$  was shown by the change in surface symmetry from  $\text{C}_{3v}$  for adsorbed, anhydrous  $\text{ClO}_4$  to  $\text{T}_d$  (tetrahedral) for fully hydrated  $\text{ClO}_4$  [27].

Energetic considerations are useful in predicting ion solvation. In the  $\text{H}_2\text{O}/\text{H}$  and  $\text{H}_2\text{O}/\text{ClO}_4$  examples above, both processes were shown to be energetically favourable, with respective free energy changes of  $-0.1\text{ eV}$  [26] and  $-1.3\text{ eV}$  [27]. In the case of  $\text{H}_2\text{O}/\text{H}/\text{Cu}(110)$ , however, the unfavourable free energy change of  $+3.6\text{ eV}$  and supporting experimental evidence lead to the conclusion that hydronium ions do not form [29,30].

An alternative method for comparing UHV and electrochemical (EC) reactions is by means of UHV–EC analogy:

$$\Phi = e(E_{\text{NHE}} + E_{\text{k}}) \quad (3)$$

in which  $\Phi$  is the work function of the adsorbate covered surface,  $e$  the magnitude of the charge of an electron,  $E_{\text{NHE}}$  the standard reduction potential, and  $E_{\text{k}}$  the so-called absolute electrode potential of a normal hydrogen electrode (referenced to a point just outside the surface of the electrolyte) [24,31]. Detailed discussions of the UHV–EC analogy have appeared in Refs. [24,31]. The absolute electrode potential has been reported as 4.4 [32,33] and 4.8 V [34,35]. Reaction (1) has a standard reduction potential of 0.342 V, meaning that reaction to the right is favoured at lower potentials. Given the different reported values of absolute electrode potentials, this standard reduction potential corresponds to a work function of 4.7 or 5.1 eV, both of which are well above the work function of  $\text{H}_2\text{O}/\text{OH}$  on Ag(110) [9,24,31]. From the UHV–EC analogy, therefore, one expects that the reaction of water with oxygen on silver will lead to the formation of hydroxide ions.

In this paper we report and examine the evidence for solvation and ionization of OH in water

adlayers on Ag(110) under cryogenic, UHV conditions. We first consider the surface solvation number as a function of OH-stabilized water coverage to propose a model of OH–H<sub>2</sub>O surface interactions. When OH ions are solvated in the water adlayers, the course of OH–H<sub>2</sub>O interactions as well as the mobility of isotopically labelled species can be followed by isotopic exchange between labelled OH groups and unlabelled H<sub>2</sub>O molecules. To test for proton exchange, we label the hydroxyl groups as OD, and to test for hydroxyl mobility, we label them as <sup>18</sup>OD. We also use a Born–Haber thermodynamic cycle to show the feasibility of OH ionization and solvation in this system.

## 2. Experimental

The experiments were carried out in a two-level, stainless-steel UHV chamber with a base pressure of  $2 \times 10^{-10}$  Torr that has been described elsewhere [26,36]. Preparation and characterization of the silver substrate have also been previously reported [37]. Temperature programmed desorption (TPD) measurements were performed with a Balzers QMG 112 mass spectrometer attached to a computer for multiple signal acquisition [38]. The heating rate was  $3 \text{ K s}^{-1}$ .

Oxygen-16 (Matheson, extra dry) was used as received. Deuterium oxide (Cambridge Isotope Laboratory, 99.9%) and oxygen-18 (Isotonec, 99.9%) were used in the isotopic exchange experiments. Water was doubly de-ionized, distilled and subjected to several freeze–thaw cycles to remove dissolved gases. Oxygen and D<sub>2</sub>O exposures were made through separate glass capillary array dosers [39]. The dosing assembly was located ca 5 mm from the sample during adsorption. Water vapour (H<sub>2</sub>O) was introduced to the crystal directly from a cone-shaped effusive doser [40] located at the upper level of the chamber. Mass spectrometer measurements detected no contamination of the H<sub>2</sub>O source by either HDO or D<sub>2</sub>O.

To prepare the surface with OD, the silver crystal was sputtered clean with Ar<sup>+</sup> ions and annealed to 773 K before each set of experiments. The substrate subsurface region was saturated with oxygen by eight to nine adsorption–desorption

cycles of <sup>16</sup>O<sub>2</sub>. The chemisorbed OD layer was prepared by first exposing the sample to O<sub>2</sub> to produce adsorbed, atomic oxygen at 270 K and then cooling it to 110 K for D<sub>2</sub>O adsorption and subsequent reaction to form OD according to Eq. (2). Next, the sample was annealed to 250 K to remove the low temperature adsorption states of water and to leave only chemisorbed OD on the surface. The experiment continued by cooling the sample back to 110 K to adsorb the H<sub>2</sub>O adlayers of study.

The <sup>18</sup>OD chemisorbed layer was prepared in a similar fashion as the OD layer, but <sup>18</sup>O<sub>2</sub> was used instead of <sup>16</sup>O<sub>2</sub> for both subsurface saturation and <sup>18</sup>OD preparation. The <sup>18</sup>OD adlayer always contained a substantial amount of <sup>16</sup>OD, however. The main source of <sup>16</sup>OD came from the reaction of D<sub>2</sub><sup>16</sup>O with <sup>18</sup>O to make the hydroxyl groups. A secondary source of <sup>16</sup>O came from subsurface oxygen [41]. Numerous adsorption–desorption cycles of <sup>18</sup>O<sub>2</sub> were performed to exchange subsurface <sup>16</sup>O by <sup>18</sup>O, but this exchange could not be completed. For the <sup>18</sup>OD experiments reported in this paper the ratio of <sup>18</sup>OD:<sup>16</sup>OD was ca 1:3. The presence of <sup>16</sup>OD does not affect the conclusion drawn from Fig. 4, which is the only use of <sup>18</sup>OD results.

The assignment for mass-to-charge (*m/e*) ratio 21 in the TPD spectra of Fig. 4 to HD<sup>18</sup>O<sup>+</sup> is based on a comparison of the relative intensity of the 21 amu peak in the TPD experiments with that produced by the mass spectrometer in the ion–molecule reactions. The mass spectrometer sensitivities in Figs. 2–4, are scaled with respect to that in Fig. 1. In separate mass spectrometric measurements of H<sub>2</sub>O, we observed relative intensities of 1:1000 for peaks 19:18 (H<sub>3</sub>O<sup>+</sup>:H<sub>2</sub>O<sup>+</sup>), and for those of D<sub>2</sub>O we observed relative intensities of 1:300 for peaks 21:20 (HD<sub>2</sub>O<sup>+</sup>:D<sub>2</sub>O<sup>+</sup>) and the same for 22:20 (D<sub>3</sub>O<sup>+</sup>:D<sub>2</sub>O<sup>+</sup>). The relative intensity of masses 21:20 in the TPD experiments of Fig. 4 is ca 1:6, which is two orders of magnitude greater than that obtained in ion–molecule reactions, and we therefore assign the signal for mass 21 to HD<sub>18</sub>O<sup>+</sup>.

Coverage calibrations for oxygen, water and hydroxyl were performed as previously described [15,42]. All coverages are reported in units of

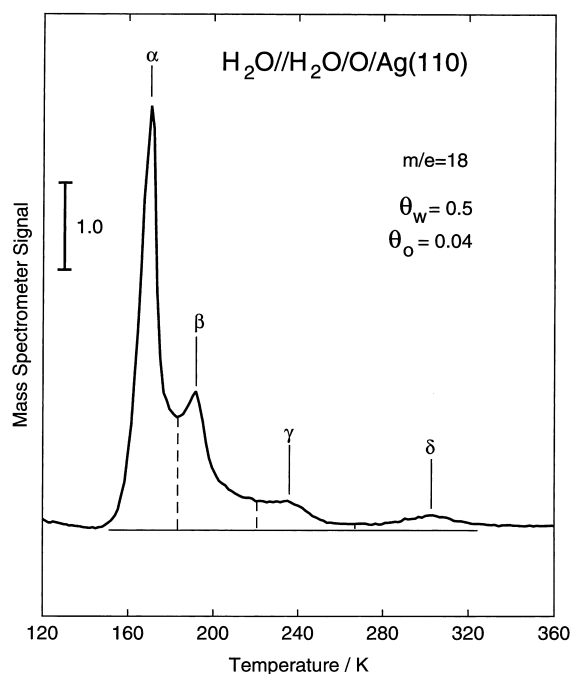


Fig. 1. TPD spectrum of water following adsorption of 0.5 ML of water onto Ag(110) at 110 K pre-covered with 0.04 ML of atomic oxygen.

monolayer (ML) based on the number of top-most silver atoms of the perfect (110) surface:  $8.45 \times 10^{14} \text{ cm}^{-2}$ .

### 3. Results

A typical TPD spectrum for water adsorbed on an oxygen-covered Ag(110) surface is shown in Fig. 1. Four desorption states were observed in agreement with previous results [4,6,8,9,11–13]. The  $\alpha$  desorption state at 170 K is the multilayer ice state. The  $\beta$ -state occurs at 190 K, and its assignment is one of the subjects of this paper. The  $\gamma$ -state at 225 K has been attributed to the formation of an  $(\text{OH})_2 \cdot \text{H}_2\text{O}$  complex with both water molecules and hydroxyl groups in direct contact with the surface [4,9]. Surface hydroxyl recombination [reverse of Reaction (2)] occurs at 300 K and is labelled the  $\delta$ -state.

To probe the H/D exchange of OH in water adlayers, surface OD groups were prepared and then covered with  $\text{H}_2\text{O}$  adlayers. In the subsequent

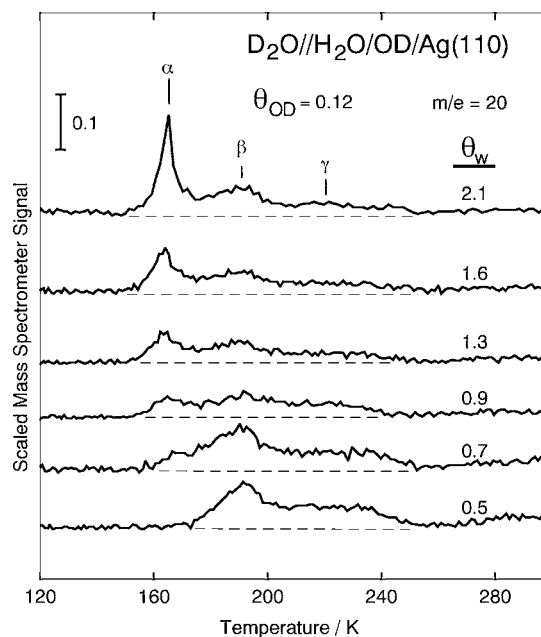


Fig. 2. TPD spectra of  $\text{D}_2\text{O}$  following adsorption of various amounts of  $\text{H}_2\text{O}$  on Ag(110) at 110 K pre-covered with 0.12 ML of OD.

TPD experiments, we detected both  $\text{D}_2\text{O}$  ( $m/e=20$ ) and  $\text{HDO}$  ( $m/e=19$ ) in all desorption states of water. Fig. 2 shows TPD spectra of  $\text{D}_2\text{O}$  following adsorption of  $\text{H}_2\text{O}$  on a surface precovered with 0.12 ML OD. The notation at the top of the figure shows the species detected to the left of the double slash and the preparation of the adlayer (in reverse order) to the right of the double slash. In all cases, the signals of both  $\text{D}_2\text{O}$  and  $\text{HDO}$  (not shown) were above the background level. At low water coverage no desorption of  $\text{D}_2\text{O}$  was observed in the  $\alpha$ -state, though the  $\alpha$ -state did appear for  $\text{H}_2\text{O}$ , as shown in Fig. 3, in which the thin line is the spectrum of  $\text{D}_2\text{O}$  and the thick line is that of  $\text{H}_2\text{O}$ . The desorption of  $\text{D}_2\text{O}$  begins to appear in the  $\alpha$ -state with 0.7 ML of  $\text{H}_2\text{O}$  (Fig. 2) and grows with increasing water coverage. Similar behaviour was observed in the TPD spectra of  $\text{HDO}$ .

The mobility of hydroxyl groups was examined by labelling them as  $^{18}\text{OD}$  to follow the migration of both hydrogen and oxygen atoms of  $^{18}\text{OD}$  in the  $\text{H}_2\text{O}$  ice layers. We observed the presence of  $\text{HD}^{18}\text{O}$  ( $m/e=21$ ) in all states of the TPD spectra

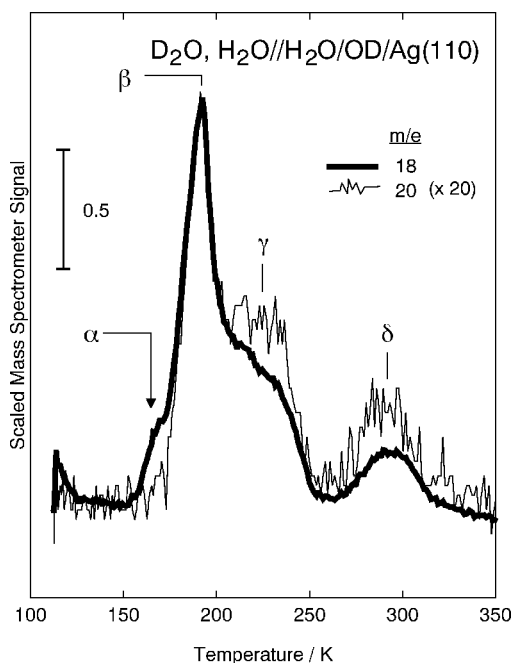


Fig. 3. TPD spectra following adsorption of 0.5 ML  $\text{H}_2\text{O}$  onto 0.12 ML OD on Ag(110) at 110 K. The thinner line is the  $\text{D}_2\text{O}$  ( $m/e=20$ ) spectrum and the thicker line is the  $\text{H}_2\text{O}$  ( $m/e=18$ ) spectrum.

as shown in Fig. 4. Desorption of  $\text{D}_2^{18}\text{O}$  ( $m/e=22$ ) was below the detection limit of our instrument.  $\text{HD}^{18}\text{O}$  desorption in the  $\alpha$ -state appears for 1.4 and 2.5 ML of  $\text{H}_2\text{O}$  coverage, but not for 0.4 ML. Similar to the results of the H/D exchange experiments, we observed an increase in the  $\alpha$ -state of  $\text{HD}^{18}\text{O}$  with increasing water coverage. The unusual distribution of water between the  $\beta$ - and  $\gamma$ -states for 0.4 ML is attributed to an insufficient number of water molecules to complete the surface saturation of hydroxyl groups. Desorption of the  $\beta$ - and  $\gamma$ -states occurs in all cases, though  $\gamma$ -state desorption is minimal at 2.5 ML  $\text{H}_2\text{O}$  coverage.

## 4. Discussion

### 4.1. Surface solvation number and OH-induced stabilization

On a clean Ag(110) surface, water desorbs at ca 165 K in the  $\alpha$ -state peak shown in Fig. 1. The

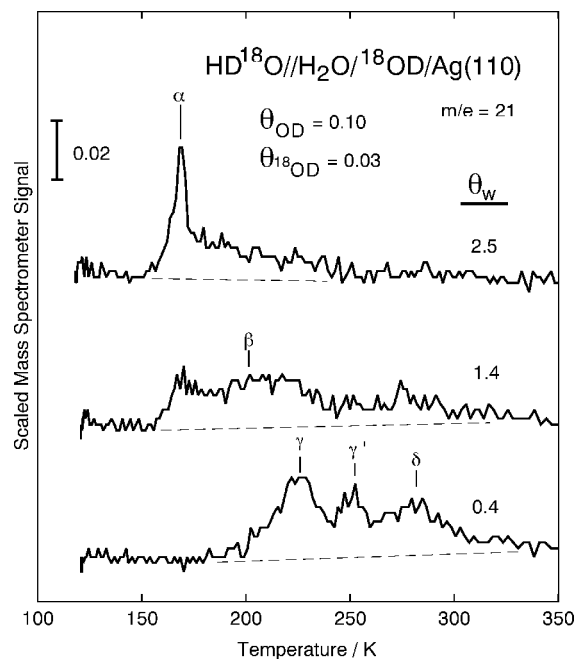


Fig. 4. TPD spectra of  $\text{HD}^{18}\text{O}$  for various  $\text{H}_2\text{O}$  coverages adsorbed onto Ag(110) at 110 K with 0.03 ML of  $^{18}\text{OD}$  and 0.10 ML OD.

presence of coadsorbed OH, however, stabilizes molecular water and the higher temperature  $\beta$  and  $\gamma$  desorption states occur. Similar stabilization of water has been observed for Ag(110) with coadsorbed F [43,44], Cl [36,45], and Br [8], and for water/oxygen coadsorption on Cu(110) [15], Ni(110) [21,22], and Pd(110) [18]. A measure to quantify the stabilization of surface water is the surface solvation number  $N_s$  given by [43]:

$$N_s = \frac{\theta_w^s}{\theta_{\text{OH}}} = \frac{\theta_\beta + \theta_\gamma}{\theta_{\text{OH}}} \quad (4)$$

where  $\theta_w^s$  is the total coverage of water stabilized by OH,  $\theta_{\text{OH}}$  is the coverage of surface OH, and  $\theta_\beta$  and  $\theta_\gamma$  are the respective coverages of water in the  $\beta$ - and  $\gamma$ -states. The surface solvation number is the total amount of water molecules stabilized by each hydroxyl group, which serves as the model anion in this case.

Fig. 5 illustrates the dependence of surface solvation number and total coverage of stabilized water on OH coverage. The open squares are the

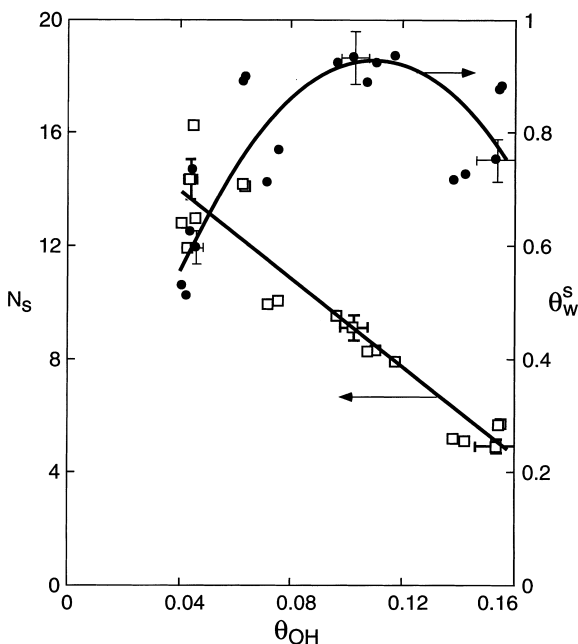


Fig. 5. Surface solvation number  $N_s$  and coverage of stabilized water  $\theta_w^s$  for  $\text{H}_2\text{O}/\text{OH}/\text{Ag}(110)$  for total water coverages of 1–2 ML.

data for solvation number, and the straight line is the best fit line through the data. The surface solvation number decreases linearly from  $14 \pm 3$  to  $5 \pm 1$  for OH coverage increasing from 0.05 to 0.15 ML. The large surface solvation number at low coverage essentially matches the value of 13 found for both  $\text{H}_2\text{O}/\text{Cl}$  [36] and  $\text{H}_2\text{O}/\text{F}$  [43] on  $\text{Ag}(110)$ , and is appreciably greater than the value of 8 found for  $\text{H}_2\text{O}/\text{O}/\text{Cu}(110)$  [15]. The filled circles in Fig. 5 show the data for the total coverage of stabilized water, and the curve through those data points is a quadratic function that follows directly upon substitution of the linear relationship of  $N_s(\theta_{\text{OH}})$  into the second equality of Eq. (4). This quantity is insensitive to the overall coverage of water, which varies between 1 and 2 ML and includes the  $\alpha$ -state. The total coverage of stabilized water increases as a function of OH coverage until it reaches a maximum of  $\theta_{w, \text{max}}^s = 0.93$  at  $\theta_{\text{OH}} = 0.11$  and then decreases at higher OH coverages. At the maximum the combined coverage of stabilized water and hydroxyl groups, 1.04 ML, is in very good agreement with the coverage expected

of a perfect hexagonal bilayer of water, 1.18 ML. Similar relationships between stabilized water and adsorbed anions have been previously observed for  $\text{H}_2\text{O}/\text{Cl}$  [36] and  $\text{H}_2\text{O}/\text{Br}$  [8]. The  $\text{H}_2\text{O}/\text{Cl}$  system also exhibits a maximum coverage of stabilized water of 1.15 ML.

The manner in which a surface hydroxyl group stabilizes so many water molecules can be rationalized by comparison to the other high surface solvation systems and to water adsorbed on fcc (110) surfaces in general. The  $\text{H}_2\text{O}/\text{Cl}/\text{Ag}(110)$  system forms a  $c(2 \times 2)$  structure, whereas the  $\text{H}_2\text{O}/\text{F}/\text{Ag}(110)$  system forms no ordered adlayer under conditions of high surface solvation. Water does not form an ordered adlayer on clean  $\text{Ag}(110)$ , but does adsorb into a  $c(2 \times 2)$  structure on  $\text{Cu}(110)$  [15],  $\text{Pd}(110)$  [18] and  $\text{Ni}(110)$  [22]. On the copper and palladium surfaces, this structure represents a distorted hexagonal bilayer, whereas on the nickel surface it represents isolated molecules. The  $c(2 \times 2)$  phase remains when water is coadsorbed with atomic oxygen on  $\text{Cu}(110)$  under conditions of high surface solvation [15].

Thus, there is a tendency for water to adopt a  $c(2 \times 2)$  structure on fcc (110) surfaces, but whether this occurs depends on a balance of forces among substrate and adsorbates [27,43,46]. The  $c(2 \times 2)$  structure for pure water on  $\text{Cu}(110)$  and  $\text{Pd}(110)$  arises from a substrate–water interaction just strong enough to distort, but not destroy, the hydrogen bonded hexagonal structure of water. For  $\text{Ni}(110)$  the substrate–water interaction is sufficiently strong to hold isolated water molecules in a  $c(2 \times 2)$  structure, whereas on  $\text{Ag}(110)$  the substrate–water interaction is so weak that water adsorbs in three dimensional, hydrogen bonded clusters with no registry to the surface.

The  $c(2 \times 2)$  pattern for the  $\text{H}_2\text{O}/\text{O}/\text{Cu}(110)$  system indicates that the hexagonal bilayer structure is not disrupted by oxygen stabilization. The  $c(2 \times 2)$  pattern for the  $\text{H}_2\text{O}/\text{Cl}/\text{Ag}(110)$  system was attributed to through-surface interactions between Cl and the affected water molecules causing a sufficient substrate–water interaction to establish an ordered adlayer, where none had existed without the Cl interaction. The absence of an ordered adlayer for the  $\text{H}_2\text{O}/\text{F}/\text{Ag}(110)$  system was attributed to the much stronger  $\text{F} \cdots \text{H}_2\text{O}$

hydrogen bonding interaction compared to that of  $\text{Cl}^- \text{H}_2\text{O}$  (1.0 versus 0.6 eV, respectively, for gas phase ion hydration) [43,47,48]. In this case strong hydrogen bonding with the coadsorbate does not allow establishment of a distorted bilayer. The stabilized water molecules may still exist in a hexagonal network – though out of registry with the substrate and hence not detectable by LEED – or as a tightly bound, three-dimensional hydration shell around the coadsorbate species.

The question of whether stabilization produces a hydrogen bonded surface network, which we call an extended surface bilayer, or a three-dimensional hydration shell applies to the  $\text{H}_2\text{O}/\text{OH}$  system as well. Like the  $\text{H}_2\text{O}/\text{F}$  system, no ordered adlayer has been detected for the  $\text{H}_2\text{O}/\text{OH}$  system under conditions of high surface solvation. Given the similar strengths of the  $\text{F}^- \dots \text{H}_2\text{O}$  and  $\text{OH}^- \dots \text{H}_2\text{O}$  interactions in the gas phase, this result also suggests that strong hydrogen bonding with OH does not permit a distorted water bilayer in registry with  $\text{Ag}(110)$ . Evidence in favour of an extended surface bilayer comes from the existence of a maximum amount of stabilized water that corresponds to a full surface bilayer. The maximum amount of stabilized water occurs for an OH coverage of 0.11 ML, for which the surface solvation number is 9 (see Fig. 5). If three-dimensional hydration shells formed, one would expect that the maximum amount of stabilized water to exceed a full perfect bilayer. That the combined coverage of stabilized water and hydroxyl groups is less than a perfect bilayer (1.04 versus 1.18 ML, respectively) indicates that:

1. the  $\text{H}_2\text{O}/\text{OH}$  coadsorption system is sensitive to complete coverage of the surface; and
2. adlayer defects prevent the full coverage expected for a perfect bilayer.

Comparison with the  $\text{H}_2\text{O}/\text{F}$  and  $\text{H}_2\text{O}/\text{Cl}$  systems, which have maximum stabilized water coverages of 1.25 [43] and 1.15 ML [36], respectively, provides further evidence to support an extended surface bilayer. These two results show that both non-ordered and ordered adlayers with high solvation numbers are limited by the coverage of a perfect bilayer. Finally, the maximum hydration numbers of 5 for the gas phase  $\text{OH}^-$  [47,48] and 4–6.6 for the aqueous  $\text{OH}^-$  [49] argue against the

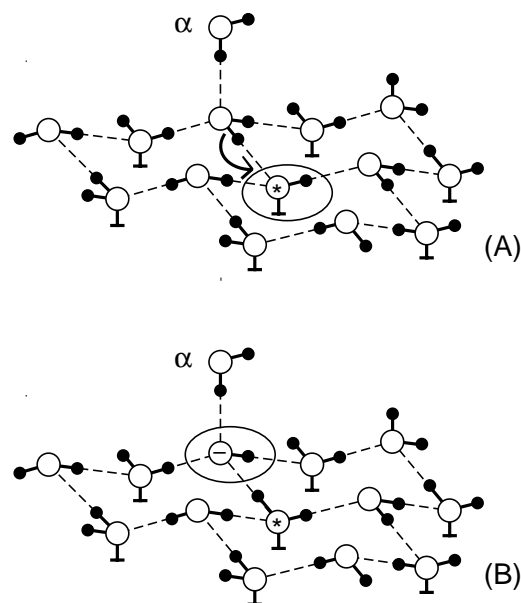


Fig. 6. Proposed extended surface bilayer model of the  $\beta$ -state for coadsorbed water and OH on  $\text{Ag}(110)$ : (A) OH group in direct contact with the surface stabilizes as many as three hexagonal rings of water molecules; (B) desorption and solvation of  $\text{OH}^-$  by proton transfer in conjunction with an  $\alpha$ -state molecule.

formation of three-dimensional hydration shells of 9–12 water molecules per surface hydroxyl group.

Fig. 6A shows an example of surface hydroxyl stabilization of water. The hydroxyl group, labelled with an asterisk, is hydrogen bonded to three hexagonal bilayer rings of water molecules. In this manner one hydroxyl group can stabilize as many as 12 water molecules (exclusive of the  $\alpha$ -state molecule shown in the figure). A similar model was proposed for the  $c(2 \times 2)$  structure of  $\text{H}_2\text{O}/\text{Cl}/\text{Ag}(110)$  [36] in which case the hexagonal rings are distorted in order to align with the  $\text{Ag}(110)$  substrate. It is also clear that unusually strong hydrogen bonding between water and either adsorbed OH (shown in the Fig. 6A) or adsorbed F (which is isoelectronic with OH) could contract or distort the hexagonal rings sufficiently to prevent alignment with the substrate. The model of Fig. 6A predicts a value of 12 for the maximum surface solvation number in agreement with the maximum hydration number of  $14 \pm 3$  at an OH coverage of 0.05 ML in Fig. 5. It is not clear whether the hydration number will continue to



increase with lower OH coverage or remain constant, as predicted by the model. We have no data for lower OH coverages, and in any case, such data would most likely be inconclusive because the error in OH coverage increases substantially with decreasing coverage and leads to very large uncertainty in the surface hydration number [36].

#### 4.2. Deuterium exchange experiments

We observed isotopic exchange in all water desorption states including the multilayer ice state. To quantify the extent of deuterium exchange in the adlayers, an approach to equilibrium in state  $i$   $\eta_i$  is defined as:

$$\eta_i = \left( \frac{\theta_i^D}{\theta_i^D + \theta_i^H} \right) \left[ \frac{\sum_i \theta_i^D}{\sum_i (\theta_i^D + \theta_i^H)} \right]^{-1} \quad (5)$$

where the term in parentheses represents the atom fraction of deuterium in state  $i$  and the term in brackets the atom fraction of deuterium in the entire adlayer. Isotopic exchange for state  $i$  is complete when  $\eta_i$  is equal to 1.

The approach to exchange equilibrium for the different desorption states as a function of water coverage is shown in Fig. 7. The solid circles, open triangles, open squares and filled diamonds represent the  $\alpha$ ,  $\beta$ ,  $\gamma$  and  $\delta$  desorption states, respectively. The lines are drawn to guide the eye. The decrease of  $\eta_i$  in the  $\delta$  state from 1.5 to 1.2 with increasing water coverage suggests incomplete exchange of deuterium out of the  $\delta$  state at low water coverage, but that the exchange approaches completion (equilibrium) when the water coverage increases. On the other hand, the increase of  $\eta_i$  from 0.5 to 1.0 for the  $\alpha$ -state suggests incomplete exchange of deuterium into the  $\alpha$ -state at low coverage. The exchange is complete only when there is ca 2.5 ML of water, thus proving that full water multilayers are necessary to achieve equilibrium exchange. In the  $\beta$ -state  $\eta_i$  remains at ca 1.0 for almost all  $H_2O$  coverages. A dashed line is drawn for the  $\gamma$ -state data, which are scattered between 1.1 and 1.3 and have no noticeable trend. For the  $\beta$ - and  $\gamma$ -states exchange appears to be complete for all water coverages. This observation

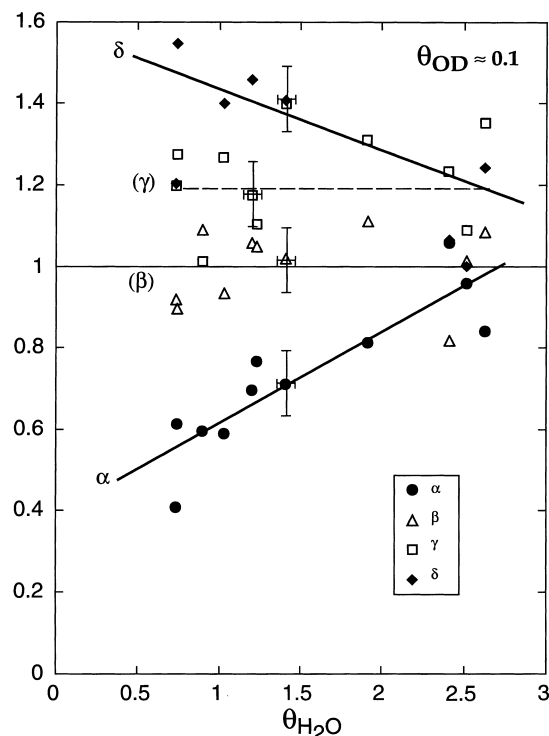


Fig. 7. Extent of deuterium exchange  $\eta_i$  as a function of water coverage for an OD coverage of 0.1 ML.

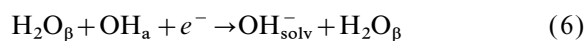
is consistent with the  $\beta$ - and  $\gamma$ -state water molecules interacting more directly with the OH groups and therefore acting as intermediates for deuterium exchange from the source ( $\delta$ -state) to the destination ( $\alpha$ -state).

#### 4.3. OH solvation and ionization

We now consider the behaviour of adsorbed OH groups in the OH/ $H_2O$  adlayer under conditions corresponding to the maximum amount of stabilized water. The situation is shown in Fig. 6 for surface OH labelled with an asterisk. In this model all of the surface water molecules are in the  $\beta$ -state as they share a hexagonal ring with the surface OH group and are bound to the surface. At the maximum stabilized water coverage the  $\alpha$ -state water molecules must reside in the second bilayer and beyond as there is no space for a water molecule to adsorb to the surface *without* interacting with the OH group. Fig. 6A shows one

$\alpha$ -state water molecule as an example. Water molecules in the  $\gamma$ -state are not present under these conditions. This follows since the  $\gamma$ -state represents an  $\text{H}_2\text{O} \cdot (\text{OH})_2$  complex [9], and the surface solvation number of 2 for the complex is inconsistent with the value of 9 for the maximum stabilized water coverage. Furthermore, the  $\gamma$ -state exhibits  $p(m \times 1)$  ( $m=2, 3, \dots$ ) LEED patterns depending on the OH coverage. For completeness, the  $\delta$ -state is represented by the surface hydroxyl group itself.

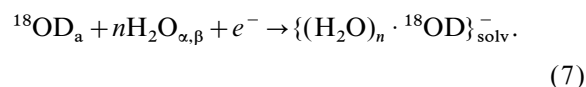
Through proton mobility [50–52] the structure in this adlayer can transform to that of Fig. 6B by virtue of the exchange between a  $\beta$ -state molecule and the OH group:



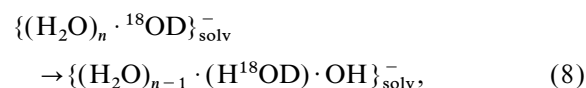
where the subscript “solv” designates an  $\text{OH}^-$  ion removed from the surface and fully solvated, and a water molecule in direct contact with the surface that may be characterized as  $\beta$  since it is a member of a ring involving an  $\text{OH}^-$  group and in contact with the surface. As shown by the isotope exchange results of Fig. 7 this process requires the presence of water multilayers, which is represented in Fig. 6 by the  $\alpha$ -state water molecule in the second bilayer.

The water adlayer depicted in Fig. 6 contains no hydrogen bond defects and thus would correspond most closely to the crystalline phase of adsorbed water. However, the conditions of water adsorption used in this work should produce an amorphous phase [53], in which a number of hydrogen bond defects would be expected. Such defects, known as Bjerrum defects [50,52], consist of “D-defects”, with two hydrogen atoms occupying a single hydrogen bond ( $\text{O}-\text{H} \cdots \text{H}-\text{O}$ ), and “L-defects”, with no hydrogen atoms occupying a hydrogen bond ( $\text{O} \cdots \text{O}$ ). Bjerrum defects provide a mechanism for hydrogen mobility in ice, which can also lead to motion of the negative charge away from the surface and into the water adlayer. Whether charge motion occurs by the direct proton hopping mechanism of Fig. 6 or by action of Bjerrum defects cannot be determined. In any event the source of the negative charge is the surface hydroxyl group, which acts as a dopant species for the water adlayer, and once removed from the surface the negative charge exists as a solvated  $\text{OH}^-$  species.

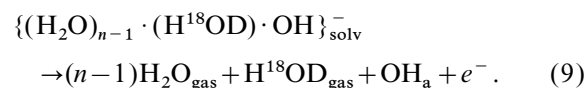
While proton mobility provides a mechanism sufficient for displacing charge from the surface and into the water adlayer, there is some evidence for direct desorption and solvation of  $\text{OH}^-$  in the ice multilayer. Experiments with  $^{18}\text{OD}$  allowed this possibility to be examined, and the presence of labelled oxygen in the  $\alpha$ -state in Fig. 4 provides the necessary evidence. These experiments correspond to the case of a fully extended surface bilayer, so that  $\alpha$ -state molecules must reside in the multilayers; they cannot contact the surface directly. The oxygen label appears in the  $\alpha$ -state whenever there is a sufficient amount of excess multilayers to stabilize and solvate a hydroxide ion. Note that the first appearance of the label in the  $\alpha$ -state occurs at a water coverage of 1.4 ML, which is enough to fill the extended surface bilayer and just begin to form excess multilayers. The label is especially evident in the  $\alpha$ -state when there is greater than one excess multilayer (top curve). This we take as evidence that  $^{18}\text{OD}$  “desorbs” from the surface to become a fully hydrated hydroxide ion. This process involves substantial reorganization of a number of molecules and may be written as:



Appearance of the  $^{18}\text{O}$  label in the  $\alpha$ -state of the TPD spectrum can be understood through subsequent conversion to molecular water by proton transfer:



followed by thermal desorption of the adlayers:



The ion motion illustrated in Eqs. (7)–(9) has recently been reported near the desorption temperature of multilayer ice [54]. Eqs. (7)–(9) denote a process of combined molecular diffusion [50–52,55] and proton exchange [56,57], processes both known to occur in bulk water ice [50–52,55] and multilayer ice films [56,57]. Furthermore, water

mobility during the amorphous–crystalline phase transition may enhance the proton exchange process. The transition has been observed to occur at 130–160 K in bulk ice [50,56,58] and at 150–160 K in multilayer surface ice [53,59].

Eq. (9) depicts the thermal desorption process, which proceeds as follows. The  $\alpha$  and  $\beta$  water molecules are removed first, after which the OH groups interact with the remaining water to form the  $\text{H}_2\text{O} \cdot (\text{OH})_2$  complex of the  $\gamma$ -state. This involves motion of the OH groups in the temperature range of 200–220 K into a  $p(m \times 1)$  structure. Both the  $\text{H}_2\text{O}/\text{Cl}$  [36] and  $\text{H}_2\text{O}/\text{F}$  [43,44] coadsorption systems exhibit similar behaviour, that is, mobility of the coadsorbate species induced by hydration with a reduced number of water molecules, during the thermal desorption process. Eq. (9) is written for a maximum temperature of 280 K as the OH groups are shown adsorbed to the surface.

The ion hydration process requires the presence of the  $\alpha$ -state and therefore may be significant in explaining the previous report of stabilization of molecular oxygen by water on Ag(110) [10]. Because molecular and atomic oxygen co-exist on Ag(110) below 170 K, adsorbed hydroxyl groups formed by Reaction (2) are involved in the interaction. Stabilization occurred only in the presence of the  $\alpha$ -state, the same condition reported for formation of fully solvated  $\text{OH}^-$ . Apparently, the solvated hydroxides have some influence on the stability of adsorbed, molecular oxygen, though the exact details remain unclear.

#### 4.4. Thermodynamic feasibility of OH ionization and solvation

The feasibility of ionization and solvation of OH can be examined with a Born–Haber analysis, shown in Fig. 8. The analysis first considers an OH group adsorbed on the Ag(110) surface and hydrogen bonded to three other water molecules. Desorption of surface OH into the gas phase requires breaking the Ag–O bond and the three hydrogen bonds. The bond strength of the former is represented by  $D_{\text{Ag-OH}}$  and remains unspecified for the present. The bond strength of the latter  $D_{\text{H}}$  can be estimated to be 0.3 eV [43] and must be multiplied by 3/2 to account for the three

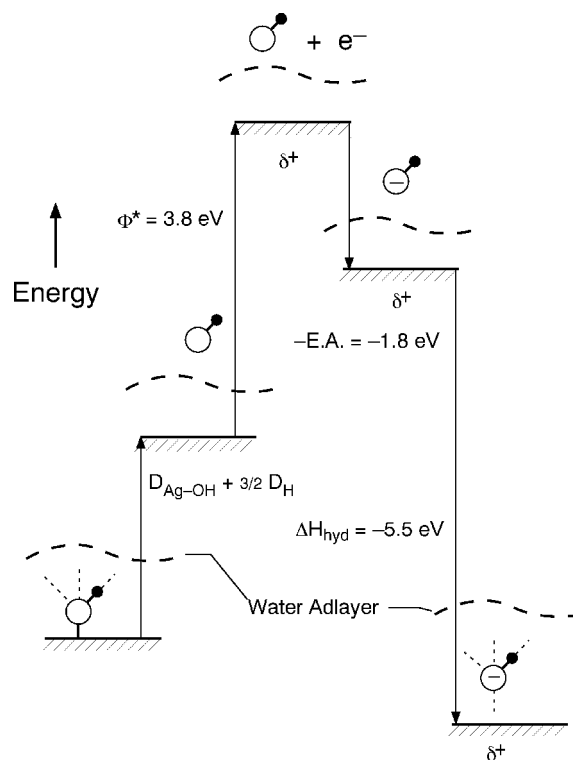


Fig. 8. Born–Haber thermodynamic cycle for solvation and desorption of surface OH as  $\text{OH}^-$ .

hydrogen bonds which are shared with three other  $\beta$  water molecules. The electron for ionizing the hydroxyl group must come from the adsorbate covered substrate, and the corresponding work is the work function of the adsorbate covered surface  $M^*$  [60]. For Ag(110) with coadsorbed water and OH this can be estimated as  $3.8 \pm 0.2$  eV [9,15,61]. The hydroxyl group then combines with the electron to form  $\text{OH}^-$  in the gas phase; the corresponding electron affinity (E.A.) is 1.8 eV [62]. The gas phase ion is then readsorbed by becoming fully hydrated by water. This results in an energy gain of the heat of hydration  $\Delta H_{\text{hyd}}$ , which is estimated to be  $-5.5$  eV [49].

The formation of hydroxyl ion in the water adlayer is thermodynamically favourable only if the free energy change of the overall reaction is less than zero:

$$D_{\text{Ag-OH}} + \frac{3}{2} D_{\text{H}} + \Phi^* - \text{E.A.} + \Delta H_{\text{hyd}} \leq 0. \quad (10)$$

Due to the low temperature of this work, we

assume that the entropic contribution to free energy is negligible, so the estimated enthalpies have been treated as free energies. Solving Eq. (10), we obtain the maximum Ag–OH bond strength for solvation to be feasible:  $D_{\text{Ag-OH}} \leq 3.05 \pm 0.2$  eV. The heat of adsorption of OH, and thus the Ag–OH bond strength, cannot be determined directly by thermal analysis, as surface OH groups decompose to form water and oxygen before they desorb. However, the upper limit of Ag–OH bond strength was estimated to be 2.0 eV [63] on the basis of a similar Born–Haber analysis. This is well below the maximum value from Eq. (10) and thus shows that the process of ionization and solvation of OH is feasible on Ag(110).

## 5. Conclusion

The combined TPD and isotopic exchange experiments have illustrated the necessary evidence for the solvation of hydroxyl group in water adlayers. The surface solvation number reaches a value of  $14 \pm 3$  at low OH coverage. An extended surface bilayer model in which surface OH stabilizes up to 12 water molecules in a hexagonal structure was presented to explain the high surface solvation. The maximum coverage of stabilized water occurred with 0.11 ML of OH, and the maximum total adlayer coverage of 1.04 ML approximates the coverage expected for a full water bilayer (1.18 ML). Isotope exchange experiments involving OD and  $^{18}\text{OD}$  showed that hydroxyl groups can ionize to  $\text{OH}^-$ , desorb from the surface, and become fully solvated in the multilayer phase. Possible mechanisms for this process include proton hopping, motion of Bjerrum defects and direct migration of  $\text{OH}^-$  away from the surface. The thermodynamic feasibility of this process was confirmed by a Born–Haber analysis. This finding of fully solvated  $\text{OH}^-$  confirms the validity of the UHV–EC analogy for characterizing surface reactions.

## Acknowledgements

The authors gratefully acknowledge the Office of Naval Research for support of this work. They

thank Bill Reinhardt, Thom Orlando and Bruce Kay for help in analyzing the results.

## References

- [1] G.D. Nagy, E.J. Casey, in: A.F.a.J.J. Lander (Ed.), *Zinc–Silver Oxide Batteries*, Wiley, New York, 1971, p. 133.
- [2] N. Sato, *Corrosion* 45 (1989) 354.
- [3] T.E. Graedel, *J. Electrochem. Soc.* 7 (1992) 1963.
- [4] E.M. Stuve, R.J. Madix, B.A. Sexton, *Surf. Sci.* 111 (1981) 11.
- [5] A. Spitzer, H. Lüth, *Surf. Sci.* 120 (1982) 376.
- [6] M.A. Barteau, R.J. Madix, *Surf. Sci.* 140 (1984) 108.
- [7] S.W. Jorgensen, A.G. Sault, R.J. Madix, *Langmuir* 1 (1985) 526.
- [8] K. Bange, T.E. Madey, J.K. Sass, *Surf. Sci.* 162 (1985) 252.
- [9] K. Bange, T.E. Madey, J.K. Sass, E.M. Stuve, *Surf. Sci.* 183 (1987) 334.
- [10] R.J. Madix, J.T. Roberts, *Surf. Sci.* 273 (1992) 121.
- [11] M. Canepa, P. Cantini, L. Mattera, E. Narducci, M. Salvietti, S. Terreni, *Surf. Sci.* 287/288 (1993) 273.
- [12] M. Canepa, P. Cantini, L. Mattera, E. Narducci, M. Salvietti, S. Terreni, *Surf. Sci.* 322 (1995) 271.
- [13] M. Canepa, P. Cantini, E. Narducci, M. Salvietti, S. Terreni, L. Mattera, *Surf. Sci.* 343 (1995) 176.
- [14] P.A. Thiel, T.E. Madey, *Surf. Sci. Rep.* 7 (1987) 211.
- [15] K. Bange, D.E. Grider, T.E. Madey, J.K. Sass, *Surf. Sci.* 137 (1984) 38.
- [16] D.A. Outka, R.J. Madix, *J. Am. Chem. Soc.* 109 (1987) 1708.
- [17] J. Fusy, R. Ducros, *Surf. Sci.* 237 (1990) 1.
- [18] J.-W. He, P.R. Norton, *Surf. Sci.* 238 (1990) 95.
- [19] R. Brousseau, T.H. Ellis, M. Morin, H. Wang, *J. Electron Spectrosc. Relat. Phenom.* 54 (55) (1990) 659.
- [20] C. Benndorf, C. Nöbl, T.E. Madey, *Surf. Sci.* 138 (1984) 292.
- [21] C. Benndorf, T.E. Madey, *Surf. Sci.* 194 (1988) 63.
- [22] B.W. Callen, K. Griffiths, U. Memmert, D.A. Harrington, S.J. Bushby, P.R. Norton, *Surf. Sci.* 230 (1990) 159.
- [23] M. Bowker, M.A. Barteau, R.J. Madix, *Surf. Sci.* 92 (1980) 528.
- [24] E.M. Stuve, N. Kishakevariam, *J. Vac. Sci. Technol. A* 11 (1993) 2217.
- [25] F.T. Wagner, T.E. Moylan, *Surf. Sci.* 206 (1988) 1.
- [26] N. Kishakevariam, E.M. Stuve, *Surf. Sci.* 275 (1992) 223.
- [27] A. Krasnopoler, E.M. Stuve, *J. Vac. Sci. Technol. A* 13 (1995) 1681.
- [28] G. Pirug, H.P. Bonzel, *Surf. Sci.* 405 (1998) 87.
- [29] D. Lackey, J. Schott, J.K. Sass, S.T. Woo, F.T. Wagner, *Chem. Phys. Lett.* 184 (1991) 277.
- [30] J. Schott, D. Lackey, J.K. Sass, *Surf. Sci.* 238 (1990) 1478.
- [31] J.K. Sass, D. Lackey, J. Schott, B. Straehler, *Surf. Sci.* 247 (1991) 239.
- [32] S. Trasatti, *Pure Appl. Chem.* 58 (1986) 955.
- [33] W.N. Hanson, G.J. Hanson, *Phys. Rev. A* 36 (1987) 1396.

- [34] R. Gomer, G. Tryson, *J. Chem. Phys.* 66 (1977) 4413.
- [35] E.R. Kötz, H. Neff, K. Muller, *J. Electroanal. Chem.* 215 (1986) 331.
- [36] N. Kizhakevariam, E.M. Stuve, R. Döhl-Oelze, *J. Phys. Chem.* 94 (1991) 670.
- [37] A. Krasnopoler, MSc. Thesis, 1992.
- [38] A.C. Liu, C.M. Friend, *Rev. Sci. Instrum.* 57 (1986) 1519.
- [39] R. Döhl-Oelze, C.C. Brown, S. Stark, E.M. Stuve, *Surf. Sci.* 210 (1988) 339.
- [40] A. Krasnopoler, N. Kizhakevariam, E.M. Stuve, *J. Chem. Soc. Faraday Trans.*, (1996)
- [41] C. Blackx, C.P.M. de Groot, P. Biloen, *Surf. Sci.* 104 (1981) 300.
- [42] H.A. Engelhardt, D. Menzel, *Surf. Sci.* 57 (1976) 591.
- [43] A. Krasnopoler, E.M. Stuve, *Surf. Sci.* 303 (1994) 355.
- [44] A. Krasnopoler, A.L. Johnson, E.M. Stuve, *Surf. Sci.* 328 (1995) 186.
- [45] J.K. Sass, K. Bange, in: M.P. Soriaga (Ed.), *Electrochemical Surface Science*, American Chemical Society, Washington, DC, 1988, p. 54.
- [46] R. Brousseau, M.R. Brustein, T.H. Ellis, *Surf. Sci.* 280 (1993) 23.
- [47] M. Arshadi, R. Yamdagni, P. Kebarle, *J. Phys. Chem.* 74 (1970) 1475.
- [48] M. Arshadi, P. Kebarle, *J. Phys. Chem.* 74 (1970) 1483.
- [49] Y. Marcus, *Ion Solvation*, Wiley, London, 1985.
- [50] P.V. Hobbs, *Ice Physics*, Clarendon Press, Oxford, 1974.
- [51] P.J. Wooldridge, J.P. Devlin, *J. Phys. Chem.* 88 (1988) 3086.
- [52] M. Fisher, J.P. Devlin, *J. Phys. Chem.* 99 (1995) 11584.
- [53] R.S. Smith, C. Huang, E.K.L. Wong, B.D. Kay, *Surf. Sci.* 367 (1996) L13.
- [54] A.A. Tsekouras, M.J. Iedema, G.B. Ellison, J.P. Cowin, *Int. J. Mass Spec. Ion Proc.* 174 (1998) 1.
- [55] M. Kunst, J. Warman, *J. Phys. Chem.* 87 (1983) 4093.
- [56] D.E. Brown, S.M. George, *J. Phys. Chem.* 100 (1996) 15460.
- [57] F.E. Livingston, G.C. Whipple, S.M. George, *J. Chem. Phys.* 108 (1998) 2197.
- [58] P. Jenniskens, D.F. Blake, *Science* 265 (1994) 753.
- [59] R.S. Smith, C. Huang, B.D. Kay, *J. Phys. Chem. B* 101 (1997) 6123.
- [60] S. Trasatti, *Surf. Sci.* 335 (1995) 1.
- [61] M. Chelvayohana, C.H.B. Mee, *J. Phys. C* 15 (1981) 2305.
- [62] D.R. Lide, *CRC Handbook of Chemistry and Physics*, CRC Press, Boston, 1990.
- [63] E.M. Stuve, S.W. Jorgensen, R.J. Madix, *Surf. Sci.* 146 (1984) 179.